www.nature.com/mi

MucosalImmunology

ARTICLE

Sphingosine 1-phosphate receptor modulator ONO-4641 stimulates CD11b$^+$Gr-1$^+$ cell expansion and inhibits lymphocyte infiltration in the lungs to ameliorate murine pulmonary emphysema

Takanori Asakura[1,2], Makoto Ishii[1], Ho Namkoong[1], Shoji Suzuki[1,2], Shizuko Kagawa[1], Kazuma Yagi[1], Takaki Komiya[3], Takafumi Hashimoto[4], Satoshi Okamori[1], Hirofumi Kamata[1], Sadatomo Tasaka[5], Akio Kihara[6], Ahmed E. Hegab[1], Naoki Hasegawa[7] and Tomoko Betsuyaku[1]

Sphingolipids play a pivotal role in the pathogenesis of chronic obstructive pulmonary disease (COPD). However, little is known about the precise roles of sphingosine-1-phosphate (S1P), a bioactive sphingolipid metabolite, and its receptor modulation in COPD. In this study, we demonstrated that the S1P receptor modulator ONO-4641 induced the expansion of lung CD11b$^+$Gr-1$^+$ cells and lymphocytopenia in naive mice. ONO-4641-expanded CD11b$^+$Gr-1$^+$ cells showed higher arginase-1 activity, decreased T cell proliferation, and lower IFN-γ production in CD3$^+$ T cells, similar to the features of myeloid-derived suppressor cells. ONO-4641 treatment decreased airspace enlargement in elastase-induced and cigarette smoke-induced emphysema models and attenuated emphysema exacerbation induced by post-elastase pneumococcal infection, which was also associated with an increased number of lung CD11b$^+$Gr-1$^+$ cells. Adoptive transfer of ONO-4641-expanded CD11b$^+$Gr-1$^+$ cells protected against elastase-induced emphysema. Lymphocytopenia observed in these models likely contributed to beneficial ONO-4641 effects. Thus, ONO-4641 attenuated murine pulmonary emphysema by expanding lung CD11b$^+$Gr-1$^+$ cell populations and inducing lymphocytopenia. The S1P receptor might be a promising target for strategies aimed at ameliorating pulmonary emphysema progression.

Mucosal Immunology (2018) 11:1606–1620; https://doi.org/10.1038/s41385-018-0077-5

INTRODUCTION

Chronic obstructive pulmonary disease (COPD) is a major cause of death worldwide.[1,2] COPD is characterized by a not-fully reversible airflow limitation, which is usually progressive and associated with chronic inflammatory and immune responses of the lungs.[3] COPD not only causes high mortality but also affects disability, health-related quality of life, and economic burden, which is further enhanced by COPD exacerbation.[1,4] The foremost pathological component of COPD is emphysematous lung destruction resulting from pathological processes initiated by cigarette smoke (CS) in most cases. Emphysema pathogenesis involves activation of a complex network of various inflammatory cells, such as neutrophils, macrophages, lymphocytes (CD4$^+$ T cells, CD8$^+$ T cells, and B cells) organized into follicles.[5] Additionally, oxidative stress, extracellular matrix proteases such as MMP-12, and alveolar cell apoptosis also contribute to alveolar destruction in emphysema.[6]

Sphingolipids are constituents of cellular membranes implicated in cellular homeostasis.[7] Notably, ceramide, a common sphingolipid structural component, plays a central role in the sphingolipid signaling pathway mediating or regulating many cellular processes, including cell cycle, apoptosis, senescence, and stress responses.[8] Elevated ceramide levels in the lungs have been reported to contribute to lung parenchymal destruction in both COPD patients[9] and an apoptosis-dependent emphysema model caused by the blockade of the vascular endothelial growth factor (VEGF) receptors in rats and mice.[10] Moreover, the signaling mediated by sphingosine-1-phosphate (S1P), a downstream pro-survival ceramide metabolite, determines cell fate, and lung remodeling responses.[11] Furthermore, plasma sphingolipids are associated with specific COPD phenotypes, such as emphysema and conditions characterized by frequent COPD exacerbation.[12] These results indicate that sphingolipid metabolism plays pivotal roles in the pathogenesis of pulmonary emphysema.

S1P receptor (S1PR) modulators have been recently used in the clinical setting. Clinical trials have revealed that S1PR modulators are beneficial in multiple sclerosis and ulcerative colitis.[13] Additionally, several clinical trials of S1PR modulators in CNS-related, autoimmune, and cancer diseases are currently in progress.[13] In mouse studies, S1PR modulators showed protective effects in various inflammatory lung disease models, including lipopolysaccharide (LPS)-induced endotoxin shock,[14] influenza viral infection,[15] and emphysema induced by VEGF receptor

[1]Division of Pulmonary Medicine, Department of Medicine, Keio University School of Medicine, Tokyo, Japan; [2]Japan Society of Promotion of Science, Tokyo, Japan; [3]Department of Biology & Pharmacology, Ono Pharmaceutical Co., Ltd, Osaka, Japan; [4]Exploratory Research Laboratories, Ono Pharmaceutical Co., Ltd, Osaka, Japan; [5]Department of Respiratory Medicine, Hirosaki University Graduate School of Medicine, Hirosaki, Japan; [6]Laboratory of Biochemistry, Faculty of Pharmaceutical Sciences, Hokkaido University, Sapporo, Japan and [7]Center for Infectious Diseases and Infection Control, Keio University School of Medicine, Tokyo, Japan
Correspondence: Makoto Ishii (ishii@keio.jp)

Received: 1 November 2017 Revised: 24 July 2018 Accepted: 1 August 2018
Published online: 16 August 2018

inhibition.[11] Fingolimod, also known as FTY720, is an agonist for S1PR1 and S1PR3-5[16] that eventually downregulates S1PR1. Therefore, fingolimod is known as an S1PR modulator. ONO-4641, used in the present study, is a novel selective agonist for S1PR1 and S1PR5, which, similarly to fingolimod, downregulates S1PR1 and contributes to lymphocytopenia.[17] Therefore, ONO-4641 is also recognized as an S1PR modulator. However, the effects of S1PR modulator administration in other emphysema models, including elastase-induced and CS-induced emphysema, have not been elucidated.

Myeloid-derived suppressor cells (MDSCs) are a heterogeneous cell population generated in the bone marrow from common myeloid progenitor cells that suppress T cell proliferation and function and expand during cancer, inflammation, and infection.[18] Murine MDSCs are defined as cells expressing both CD11b and Gr-1 markers that inhibit T cell activity.[18] It has been previously shown that the S1PR modulator fingolimod ameliorates chronic graft-versus-host disease[19] and immunological hepatic injury[20] in mice through stimulation of MDSC expansion.

In the present study, we used mouse models of COPD, namely porcine pancreatic elastase (PPE)-induced and CS-induced emphysema, and COPD exacerbation generated by pneumococcal infection on the background of elastase-induced emphysema, to examine the effects of ONO-4641, a novel selective agonist of S1PR1/S1PR5 and a functional S1PR1 suppressor.[17] We showed that ONO-4641 ameliorated pulmonary emphysema by augmenting the expansion of immunomodulatory MDSC-like CD11b$^+$Gr-1$^+$ cells and by inhibiting lymphocyte infiltration in the lungs.

RESULTS

ONO-4641 inhibits lung lymphocyte infiltration and causes the expansion of CD11b$^+$Gr-1$^+$ cells

We first examined whether the S1PR modulator ONO-4641 modulates known immune cell populations in naive wild-type (WT) mice. The mice were intragastrically administered with ONO-4641 (0.3 mg/kg) daily for 7 days, and single-cell suspensions prepared from the lungs and the spleen were analyzed by flow cytometry the day after the last administration. To determine the effect of ONO-4641 on major immune cell populations, we compared the numbers of B cells (B220$^+$), NK cells (CD3$^-$NK1.1$^+$), γδT cells (CD3$^+$γδT$^+$), and T lymphocytes (CD4$^+$ and CD8$^+$) in both the lungs and the spleen of vehicle- and ONO-4641-treated mice. The numbers of lymphocytes, except for that of NK1.1$^+$ cells in the lungs, were significantly lower in ONO-4641-treated animals (Fig. 1a, b). Notably, ONO-4641 caused a significant expansion of splenic and lung CD11b$^+$Gr-1$^+$ cell populations in naive mice by 2.2-fold and 2.0-fold, respectively (Fig. 1c, d). In addition, ONO-4641 administration decreased the numbers of B lymphocytes (B220$^+$) and T lymphocytes (CD4$^+$ and CD8$^+$), and increased the CD11b$^+$Gr-1$^+$ cell population in a time-dependent and dose-dependent manner (Supplementary Figure S1a–d and S2a-d). Previous studies have demonstrated that MDSCs, which are characterized by CD11b$^+$Gr-1$^+$ surface marker expression, consist of two major subsets: monocytic MDSCs (CD11b$^+$Ly-6G$^-$Ly-6C$^+$ cells) and granulocytic MDSCs (CD11b$^+$Ly-6G$^+$Ly-6C^{low} cells).[18] We confirmed that ONO-4641 stimulated the expansion of both of these CD11b$^+$Gr-1$^+$ cell populations, and the Ly-6C:Ly-6G ratio was found to be ~1:1 (Fig. 1e). That ratio was also around 1:1 in vehicle-treated CD11b$^+$Gr-1$^+$ cells (data not shown). Cytospin examination indicated that CD11b$^+$Ly-6G$^-$Ly-6C$^+$ and CD11b$^+$Ly-6G$^+$Ly-6C^{low} cells displayed monocytic and granulocytic morphology, respectively (Fig. 1f, g).

Previous human and animal studies have suggested that various sphingolipid signaling pathway modulators might have promising therapeutic potential; ceramide-1-phosphate (C1P), an important ceramide metabolite, had a protective effect against CS-induced airway inflammation.[21] Therefore, we evaluated how various modulators of the sphingolipid pathway, including ONO-4641, affected the number of CD11b$^+$Gr-1$^+$ cells. Importantly, ONO-4641 (a selective agonist of S1PR1/S1PR5 and a functional S1PR1 suppressor)[17] and CYM-5442 (a selective S1PR1 agonist and a functional S1PR1 suppressor)[22] increased the percentage and number of lung and splenic CD11b$^+$Gr-1$^+$ cells, whereas another S1PR1-selective agonist, SEW2871, as well as C8-C1P and C16-C1P, had no effect (Fig. 1h, i). Furthermore, treatment with ONO-4641 or CYM-5442 decreased the numbers of B lymphocytes (B220$^+$) and T lymphocytes (CD4$^+$ and CD8$^+$), whereas SEW2871 decreased only the number of CD4$^+$ lymphocytes in the lungs (Supplementary Figure S3a–c). Lung CD11b$^+$Gr-1$^+$ cells from ONO-4641-treated mice showed lower S1PR1 gene expression and higher S1PR5 gene expression compared with that from vehicle-treated mice (Fig. 1j). Taken together, these results suggest that S1PR1 functional antagonism causes the expansion of CD11b$^+$Gr-1$^+$ cells, although there is a possibility that S1PR5 agonism also contributes to this effect.

ONO-4641-expanded CD11b$^+$Gr-1$^+$ cells exhibit anti-inflammatory properties

To further characterize the phenotype of ONO-4641-expanded CD11b$^+$Gr-1$^+$ cells, we initially performed arginase activity and carboxyfluorescein succinimidyl ester (CFSE) T cell proliferation assays in the presence of sorted splenic CD11b$^+$Gr-1$^+$ cells obtained from vehicle-treated and ONO-4641-treated mice. We found a significant increase in the arginase activity of ONO-4641-expanded CD11b$^+$Gr-1$^+$ cells as compared to that of CD11b$^+$Gr-1$^+$ cells from vehicle-treated mice (Fig. 2a). Moreover, the histogram of CFSE intensity in CD3$^+$ T cells co-cultured with ONO-4641-expanded CD11b$^+$Gr-1$^+$ cells shifted to the right along the *X*-axis compared to the pattern seen in CD3$^+$ T cells co-cultured with CD11b$^+$Gr-1$^+$ cells from control animals (Fig. 2b, c), indicating that ONO-4641-expanded CD11b$^+$Gr-1$^+$ cells attenuated CD3$^+$ T cell proliferation. These findings in ONO-4641-expanded CD11b$^+$Gr-1$^+$ cells were consistent with the features of MDSCs,[18] suggesting that ONO-4641-expanded CD11b$^+$Gr-1$^+$ cells were MDSC-like cells.

We next examined ONO-4641-expanded splenic CD11b$^+$Gr-1$^+$ cells for the presence of various surface markers reported to be expressed on MDSCs and/or myeloid cells, including CD244,[23] CD49d,[24] Sca-1,[25] CCR2,[25] CX3CR1,[26] CXCR2,[25] CXCR4,[25] CXCR5,[27] CD80,[25] CD31,[28] CD62L,[25] ICAM-1,[29] MHC class II,[25] CD115/M-CSFR,[25] IL-4Rα,[25] CTLA-4,[30] CD40,[27] and PD-L1[31]. Notably, CD244 expression was higher in ONO-4641-expanded CD11b$^+$Gr-1$^+$ cells than in vehicle-treated CD11b$^+$Gr-1$^+$ cells (Supplementary Figure S4; data of the other markers are not shown).

To confirm that some ONO-4641-expanded CD11b$^+$Gr-1$^+$ (i.e., CD11b$^+$Ly-6G$^-$Ly-6C$^+$) cells are monocytic MDSCs but not M2 macrophages, the gene expression of arginase-1 (*Arg1*), IL-10 (*Il10*), Ym-1(*Chi3l3*), CD206 (*Mrc1*), and FIZZ-1 (*Retnla*) (all M2 macrophage marker genes);[32–35] *Klf4* (a critical regulator of M2 macrophage polarization);[36] and *Nos2, Tnfa, Il6*, and *Il1b* (all M1 macrophage marker genes)[32] was measured. Although some M2 macrophage-related genes, including *Arg1, Il10, Chi3l3, Mrc1*, and *Klf4*, were significantly upregulated in ONO-4641-expanded CD11b$^+$Gr-1$^+$ cells as compared to control cells, *Arg1* and *Il10* are also known to be major molecules secreted by MDSCs[18] and the magnitude of the difference was relatively modest. *Retn1a*, a major M2 macrophage marker gene,[34,35] was not upregulated in ONO-4641-expanded CD11b$^+$Gr-1$^+$ cells as compared to control cells. In addition, *Nos2*, *Tnfa*, *Il6*, and *Il1b* were also significantly upregulated in ONO-4641-expanded CD11b$^+$Gr1$^+$ cells, which is inconsistent with the notion that ONO-4641-expanded CD11b$^+$Gr1$^+$ cells are M2 macrophages.

To further investigate cellular function of these cell populations in vitro, murine alveolar macrophage MH-S cells were co-cultured with CD11b$^+$Gr-1$^+$ cells from ONO-4641-treated or vehicle-treated mice and stimulated with LPS. ONO-4641-expanded CD11b$^+$Gr-1$^+$

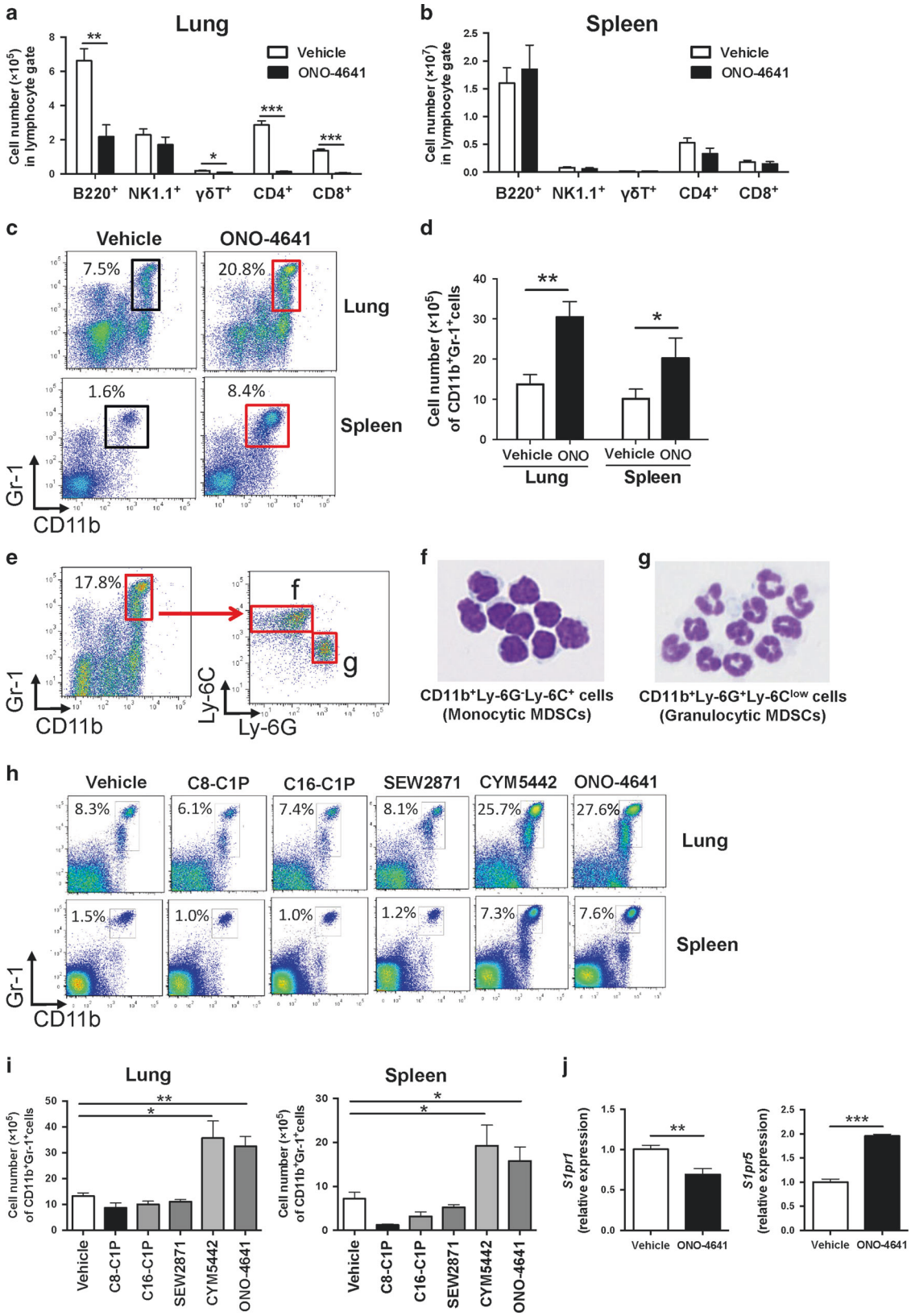

cells suppressed pro-inflammatory cytokine TNF-α production (Fig. 2e). In addition, $CD3^+$ T cells were co-cultured with $CD11b^+Gr\text{-}1^+$ cells from ONO-4641-treated or vehicle-treated mice in the presence of anti-CD3 and anti-CD28 antibodies for 72 h, and the interferon-γ (IFN-γ) level was measured by intracellular flow cytometry staining. ONO-4641-expanded $CD11b^+Gr\text{-}1^+$ cells suppressed IFN-γ production in $CD3^+$ T cells (Fig. 2f, g). Collectively, these in vitro results indicate that ONO-4641-expanded $CD11b^+Gr\text{-}1^+$ cells potentiated anti-inflammatory MDSC-like properties by regulating cytokine production.

Fig. 1 ONO-4641 stimulates expansion of $CD11b^+Gr\text{-}1^+$ cells in naive mice. **a**, **b** Quantification of major lymphocyte populations, including $B220^+$, $CD3^-NK1.1^+$, $CD3^+\gamma\delta T^+$, $CD3^+CD4^+$, and $CD3^+CD8^+$, in the lungs (**a**) and spleen (**b**) from mice intragastrically treated with vehicle or ONO-4641 (0.3 mg/kg/day) for 7 consecutive days ($n = 4$ in each group). Data are presented as the mean ± SEM. $^*P < 0.05$; $^{**}P < 0.01$; $^{***}P < 0.001$. **c**, **d** Representative two-parameter histograms (**c**) and quantification of $CD11b^+Gr\text{-}1^+$ cells in the lungs and spleen from mice intragastrically treated with vehicle or ONO-4641 (0.3 mg/kg/day) for 7 consecutive days. ($n = 4$ in each group). Data are presented as the mean ± SEM. $^*P < 0.05$; $^{**}P < 0.01$. **e** ONO-4641-expanded $CD11b^+Gr\text{-}1^+$ cells were divided into two populations: $CD11b^+Ly\text{-}6G^-Ly\text{-}6C^+$ cells (monocytic myeloid-derived suppressor cell (MDSC)-like cells) and $CD11b^+Ly\text{-}6G^+Ly\text{-}6C^{low}$ cells (granulocytic MDSC-like cells) ($n = 3$–4 in each group). **f**, **g** Representative cytospin images of $CD11b^+Ly\text{-}6G^-Ly\text{-}6C^+$ cells (monocytic MDSC-like cells) (**f**) and $CD11b^+Ly\text{-}6G^+Ly\text{-}6C^{low}$ cells (granulocytic MDSC-like cells) ($n = 3$–4 in each group) (**g**). **h** Representative two-parameter histograms of $CD11b^+Gr\text{-}1^+$ cells in the lungs and spleen from mice treated intragastrically or intraperitoneally with vehicle, C8-C1P (40 μg/kg/day), C16-C1P (50 μg/kg/day), SEW2871 (1 mg/kg/day), CYM-5442 (3 mg/kg/day), or ONO-4641 (0.3 mg/kg/day) for 7 consecutive days ($n = 4$ in each group). **i** Quantification of $CD11b^+Gr\text{-}1^+$ cells in the lungs and spleen from mice treated intragastrically or intraperitoneally with vehicle or the indicated molecules for 7 days ($n = 4$ in each group). Data are presented as the mean ± SEM. **j** *S1pr1* and *S1pr5* expression in $CD11b^+Gr\text{-}1^+$ cells sorted from the lungs of vehicle-treated or ONO-4641-treated mice (Day 7). ($n = 3$ in each group). Data are presented as the mean ± SEM. $^{**}P < 0.01$; $^{***}P < 0.001$

ONO-4641 expanded $CD11b^+Gr\text{-}1^+$ cells through the ERK pathway

To explore the mechanism underlying ONO-4641-induced $CD11b^+Gr\text{-}1^+$ cell expansion, we focused on known inducers of S1PR1 downstream signaling, including the ERK and p38 mitogen-activated protein (MAP) kinase pathway.[37,38] Phosphorylated ERK (Fig. 2h), but not phosphorylated p38 MAPK (data not shown), was upregulated in ONO-4641-expanded $CD11b^+Gr\text{-}1^+$ cells compared to vehicle-treated $CD11b^+Gr\text{-}1^+$ cells. To investigate the role of the ERK pathway on induction of $CD11b^+Gr\text{-}1^+$ cells by ONO-4641, mice were administered the MEK/ERK inhibitor U0126 30 min before ONO-4641 treatment once a day for 7 consecutive days. Notably, treatment with U0126 significantly reduced the absolute number of $CD11b^+Gr\text{-}1^+$ cells in the lungs (Fig. 2i) without any change in lymphocytopenia (Supplementary Figure S5). These results support the notion that the ERK pathway, at least in part, contributes to the ONO-4641-mediated expansion of the $CD11b^+Gr\text{-}1^+$ cell population.

ONO-4641 ameliorates airway inflammation in a mouse model of short-term cigarette smoke exposure

In a short-term cigarette smoke (CS) exposure experiment, mice were treated with vehicle or ONO-4641 at 1 h before CS administration for 60 min, once a day for 3 consecutive days. Then, we performed a histopathological examination and measured cell numbers, assessed cell differentiation, and determined cytokine levels in bronchoalveolar lavage fluid (BALF). CS exposure for 3 consecutive days resulted in increased cell infiltration (Fig. 3a). Higher numbers of leukocytes, including both neutrophils and macrophages (Fig. 3b), and increased levels of pro-inflammatory cytokines (TNF-α, IL-6, IL-1β, CXCL1, and CXCL2) in BALF (Fig. 3c) were observed in CS-exposed mice compared to the corresponding levels in controls exposed to normal air. Administration of ONO-4641 1 h prior to daily CS exposure ameliorated inflammation as shown by a decrease in the numbers of neutrophils and macrophages and reduced cytokine levels in BALF (Fig. 3b, c). Moreover, we observed a lower number of CS-induced neutrophils and lower levels of several cytokines (IL-1β, CXCL1, and CXCL2) in BALF when mice were administered ONO-4641 after CS exposure over a period of 3 days (Fig. 3d, e). Thus, ONO-4641 not only prevented but also treated early stages of established CS-induced lung inflammation.

ONO-4641 ameliorates elastase-induced emphysema

We studied the effects of ONO-4641 on COPD in a different emphysema model generated by intratracheal instillation of porcine pancreatic elastase. Elastase-induced emphysema is characterized by a substantial infiltration of neutrophils and macrophages within 24 h, followed by lymphocyte infiltration, which destroys the alveolar wall and enlarges airspace, mimicking human emphysema.[6] ONO-4641 dramatically inhibited airway space enlargement and reduced the percentage of low-attenuation area (LAA) and the mean linear intercept (Lm) measured at 28 days after elastase instillation (Fig. 4a–d). Examination of BALF elastase-induced emphysema revealed a significant decrease in the numbers of leukocytes (neutrophils and macrophages) (Fig. 4e) and levels of pro-inflammatory cytokines (TNF-α and IL-6) at the indicated time points (Fig. 4f). In addition, we examined the expression of MMP-12, a protease involved in emphysema progression[6] that is mainly produced by macrophages in the lungs.[6,39] Co-staining for MMP-12 and the macrophage marker lectin revealed that the number of $MMP\text{-}12^+lectin^+$ cells was lower in the ONO-4641-treated group than in the vehicle-treated group (Fig. 4g).

Flow cytometry analysis revealed that ONO-4641 accelerated elastase-dependent expansion of $CD11b^+Gr\text{-}1^+$ cells, including $CD11b^+Ly\text{-}6G^-Ly\text{-}6C^+$ and $CD11b^+Ly\text{-}6G^+Ly\text{-}6C^{low}$ cells, in the lungs (Fig. 4h, i). Additionally, the numbers of $B220^+$, $CD4^+$, and $CD8^+$ lymphocytes were significantly decreased in ONO-4641-treated mice compared with their numbers in vehicle-treated mice (Fig. 4j).

To investigate the role of the $CD11b^+Gr\text{-}1^+$ cell population in the elastase-induced emphysema model, we adoptively transferred $CD11b^+Gr\text{-}1^+$ cells isolated from ONO-4641-treated or vehicle-treated mice to elastase-challenged recipient mice. Adoptive transfer of ONO-4641-expanded $CD11b^+Gr\text{-}1^+$ cells dramatically inhibited airway space enlargement (Fig. 4k, l), indicating that ONO-4641-expanded $CD11b^+Gr\text{-}1^+$ cells had a protective effect against elastase-induced emphysema. The number of neutrophils was significantly decreased, while the number of macrophages was significantly increased in the group in which ONO-4641-expanded $CD11b^+Gr\text{-}1^+$ cells were adoptively transferred (Fig. 4m). There were no significant differences in cytokine production, including TNF-α, IL-6, IL-1β, CXCL1, and CXCL2, in BALF in both the adoptively transferred vehicle-treated group and the ONO-4641-expanded $CD11b^+Gr\text{-}1^+$ cell-treated group (Fig. 4n).

ONO-4641 ameliorates chronic CS-induced emphysema

We also studied the effects of ONO-4641 on COPD using a different and more clinically relevant emphysema model generated by nose-only exposure to CS as previously described.[40] In this model, the infiltration of inflammatory and immune cells and airspace enlargement after prolonged exposure for more than 3 months resemble the responses observed in humans. ONO-4641 administration attenuated airway space enlargement (Fig. 5a) and also reversed the pathological effects on Lm (Fig. 5b), destructive index (DI) (Fig. 5c), end-expiratory lung volume (Supplementary Figure S6a), and average CT value (Supplementary Figure S6b). The CT histogram curve measured at 3 months after CS exposure in the lungs of mice with ONO-4641 treatment was shifted toward that of vehicle-treated control mice exposed to normal air (Supplementary Figure S6c), confirming that ONO-4641 attenuated alveolar destruction in CS-induced emphysema. Examination of BALF from ONO-4641-treated mice with CS-induced

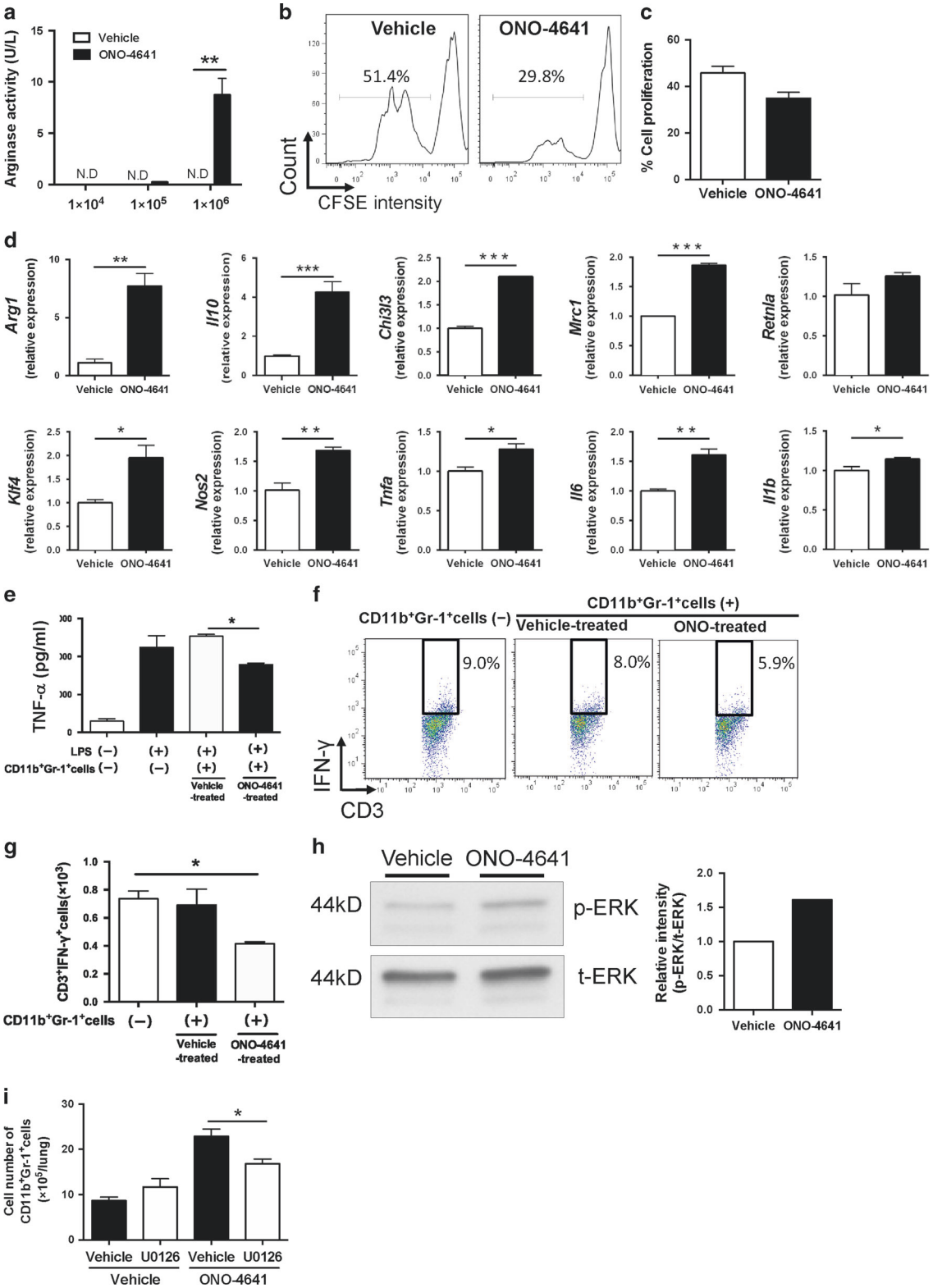

emphysema revealed significantly lower numbers of leukocytes (neutrophils, macrophages, and lymphocytes) compared to those observed in the BALF of vehicle-treated mice with emphysema (Fig. 5d). In addition, we observed comparable levels of several cytokines (TNF-α, IL-6, IL-1β, CXCL1, and CXCL2) in BALF from ONO-4641-treated and vehicle-treated mice with CS-induced emphysema (Fig. 5e).

Lymphocytopenia and expansion of the $CD11b^{+}Gr\text{-}1^{+}$ cell population in the lungs of mice with CS-induced emphysema

To further investigate the mechanism underlying the protective effects of ONO-4641 in CS-induced emphysema, we next examined immune cell populations in the lungs of CS-exposed mice. Flow cytometry analysis revealed that ONO-4641 significantly decreased the number of various lymphocyte subsets, including B cells

Fig. 2 ONO-4641-expanded CD11b$^+$Gr-1$^+$ cells displayed an immunosuppressive phenotype. **a** Arginase activity detected by CD11b$^+$Gr-1$^+$ cells sorted from vehicle-treated and ONO-4641 -treated (0.3 mg/kg/day for 7 consecutive days) mice ($n = 3$ in each group). Data are presented as the mean ± SEM. $^{**}P < 0.01$. The numbers on the *X*-axis denote the number of CD11b$^+$Gr-1$^+$ cells. **b**, **c** Representative two-parameter histograms (**b**) and percentage of cell proliferation (**c**) determined in the proliferation assay for CD3$^+$ T cells co-cultured with an equal number (1×10^5) of vehicle- or ONO-4641-expanded CD11b$^+$Gr-1$^+$ cells by the carboxyfluorescein succinimidyl ester (CFSE) method. Data shown are as the mean ± SEM, and are representative of three independent experiments performed in triplicate. **d** Expression of *Arg1*, *Il10*, *Chi3l3*, *Mrc1*, *Retnla*, *Klf4*, *Nos2*, *Tnfa*, *Il6*, and *Il1b* in CD11b$^+$Gr-1$^+$ cells sorted from the lungs of vehicle-treated or ONO-4641-treated mice (Day 7) ($n = 3$–4 in each group). Data are presented as the mean ± SEM. $^{**}P < 0.01$; $^{***}P < 0.001$. **e** TNF-α levels in the supernatant of the medium, in which MH-S macrophages were cultured with or without an equal number (5×10^5) of vehicle-treated or ONO-4641-expanded CD11b$^+$Gr-1$^+$ cells ($n = 3$ in each group). Data are presented as the mean ± SEM. $^{*}P < 0.05$. **f**, **g** Representative two-parameter histograms (**f**) and quantification (**g**) of intracellular detection of IFN-γ in CD3$^+$ T cells from the spleen after co-culture with or without equal numbers (5×10^5) of vehicle-treated or ONO-4641-expanded CD11b$^+$Gr-1$^+$ cells. Data shown are representative of three independent experiments performed in triplicate. **h** Representative immunoblotting of phosphorylated (p)-ERK (Thr202/Tyr204). Total (t)-ERK was used as the loading control. Relative band intensities were determined by densitometry analysis. **i** Quantification of CD11b$^+$Gr-1$^+$ cells in the lungs from mice intraperitoneally treated with MEK/ERK inhibitor U0126 (5 mg/kg) or control. At 30 min after treatment, mice were subsequently intragastrically treated with vehicle or ONO-4641 (0.3 mg/kg/day) once a day for 7 consecutive days. ($n = 4$–5 in each group). Data are presented as the mean ± SEM. $^{*}P < 0.05$

(B220$^+$), CD4$^+$ and CD8$^+$ T lymphocytes, NK cells (CD3$^-$NK1.1$^+$), and γδT cells (CD3$^+$γδT$^+$), compared to their levels in vehicle-treated CS-exposed controls (Fig. 6a). In addition, we examined the expression of MMP-12. Co-staining for MMP-12 and the macrophage marker F4/80 revealed that the number of MMP-12$^+$F4/80$^+$ cells was comparable between vehicle- and ONO-4641-treated groups (Fig. 6b). *Mmp12* mRNA expression in the lungs tended to be lower in the lungs of ONO-4641-treated mice, but the effect did not reach statistical significance (Fig. 6c). In addition, CS exposure enhanced the formation of peribronchovascular cell clusters (Fig. 6d), and the number of cell clusters in the lungs of ONO-4641-treated mice was significantly lower than that in vehicle-treated mice (Fig. 6e). These results indicate that lower numbers of peribronchovascular cell clusters likely contributed to the protective effects of ONO-4641 in the CS-induced emphysema mouse model. In addition, ONO-4641 accelerated CS-dependent expansion of CD11b$^+$Gr-1$^+$ cells in the lungs (Fig. 6f, g), which likely also contributed to the protective effects of ONO-4641, as in the case of elastase-induced emphysema (Fig. 4).

ONO-4641 ameliorates emphysema progression in elastase-treated mice after pneumococcal infection

We further studied the effects of ONO-4641 in a COPD exacerbation model generated by pneumococcal infection in mice with elastase-induced emphysema as previously described.[39] This model is characterized by an elevated number of inflammatory cells and increased MMP-12 production in the lungs, as well as enhanced emphysema progression, similar to the response observed in human COPD exacerbation.[41] ONO-4641 administration (0.3 mg/kg once a day at 1 h after pneumococcal infection for 14 days) inhibited emphysema progression and reduced delta LAA measured at 14 days after pneumococcal infection (Fig. 7a). The numbers of leukocytes (Fig. 7b) and neutrophils (Fig. 7c), but not of macrophages (Fig. 7d), in BALF obtained from mice with pneumococcal infection after elastase injection were lower in the ONO-4641-treated group than in the vehicle-treated control. The bacterial load in lung lysates, but not in BALF or blood, from ONO-4641-treated mice 4 days after pneumococcal infection was lower than that in vehicle-treated mice (Fig. 7e). Flow cytometry analysis revealed that ONO-4641 accelerated pneumococcal infection-dependent expansion of CD11b$^+$Gr-1$^+$ cells in the lungs (Fig. 7f, g). We subsequently tried to distinguish ONO-4641-expanded CD11b$^+$Gr-1$^+$ cells from pneumococcus-induced inflammatory granulocytes, which also express CD11b and Gr-1, by using an MDSC marker. As expected, CD244 was highly expressed by ONO-4641-expanded CD11b$^+$Ly-6G$^+$Ly-6C^{low} cells (Fig. 7h), suggesting that these cells likely obtained an MDSC-like phenotype and contributed to the beneficial effects of ONO-4641. Additionally, ONO-4641 significantly decreased the numbers of B lymphocytes (B220$^+$ cells), CD4$^+$, and CD8$^+$ T lymphocytes induced by pneumococcal infection in elastase-treated mice (Fig. 7i). Because we previously reported that both T and B lymphocytes express MMP-12 in this model,[39] we measured the MMP-12 level in these cells. We confirmed that *Mmp12* mRNA was upregulated in B lymphocytes (B220$^+$ cells), CD4$^+$, and CD8$^+$ T lymphocytes. Furthermore, ONO-4641 administration decreased *Mmp12* mRNA expression in B lymphocytes (B220$^+$ cells) and CD4$^+$ T lymphocytes in the lungs of pneumococcus-infected mice at day 4 (Fig. 7j), suggesting that lower levels of MMP-12-expressing lymphocytes also contributed to the attenuation of emphysema progression. In addition, ONO-4641 treatment significantly decreased the number of apoptotic cells (Fig. 7k, l), suggesting that ONO-4641 played a protective role at least in part by decreasing apoptosis in elastase-treated mice after pneumococcal infection.

DISCUSSION

In the present study, we report that the S1PR modulator ONO-4641 exerted anti-inflammatory effects in mouse models of COPD, namely elastase-induced and CS-induced emphysema, and prevented pneumococcal infection-induced exacerbation of COPD. In these models, ONO-4641 administration attenuated the recruitment of leukocytes, including neutrophils, macrophages, and lymphocytes, and the production of pro-inflammatory cytokines. Notably, we demonstrated that ONO-4641 stimulated the expansion of immunomodulatory CD11b$^+$Gr-1$^+$ cells in mouse COPD models, possibly contributing to its beneficial effects. In addition, the molecular mechanism of expansion of CD11b$^+$Gr-1$^+$ cells was at least in part dependent on the ERK signaling pathway.

The S1P/S1PR axis affects a variety of inflammatory immune responses and is implicated in a broad range of diseases, including cancer and inflammatory disorders such as atherosclerosis, inflammatory bowel disease, rheumatic arthritis, acute respiratory distress syndrome, and asthma.[42] The protective roles of S1P/S1PR modulators, widely reported in vivo using translational mouse models of human diseases, have been ascribed to various mechanisms. The main mechanism was thought to be drug-induced downregulation of cell surface S1PR1, in lymphocytes through functional antagonism, which causes lymphocytopenia and immunosuppression. These effects could be used for the treatment of autoimmune diseases such as multiple sclerosis and inflammatory bowel disease.[13] Moreover, previous studies have revealed that S1PR modulation enhanced endothelial barrier protection against acute lung injury in vivo.[43] Our studies indicate that in addition to lymphocytopenia, a novel unique cell population, ONO-4641-expanded CD11b$^+$Gr-1$^+$ cells, may also have an important role in counteracting emphysema progression.

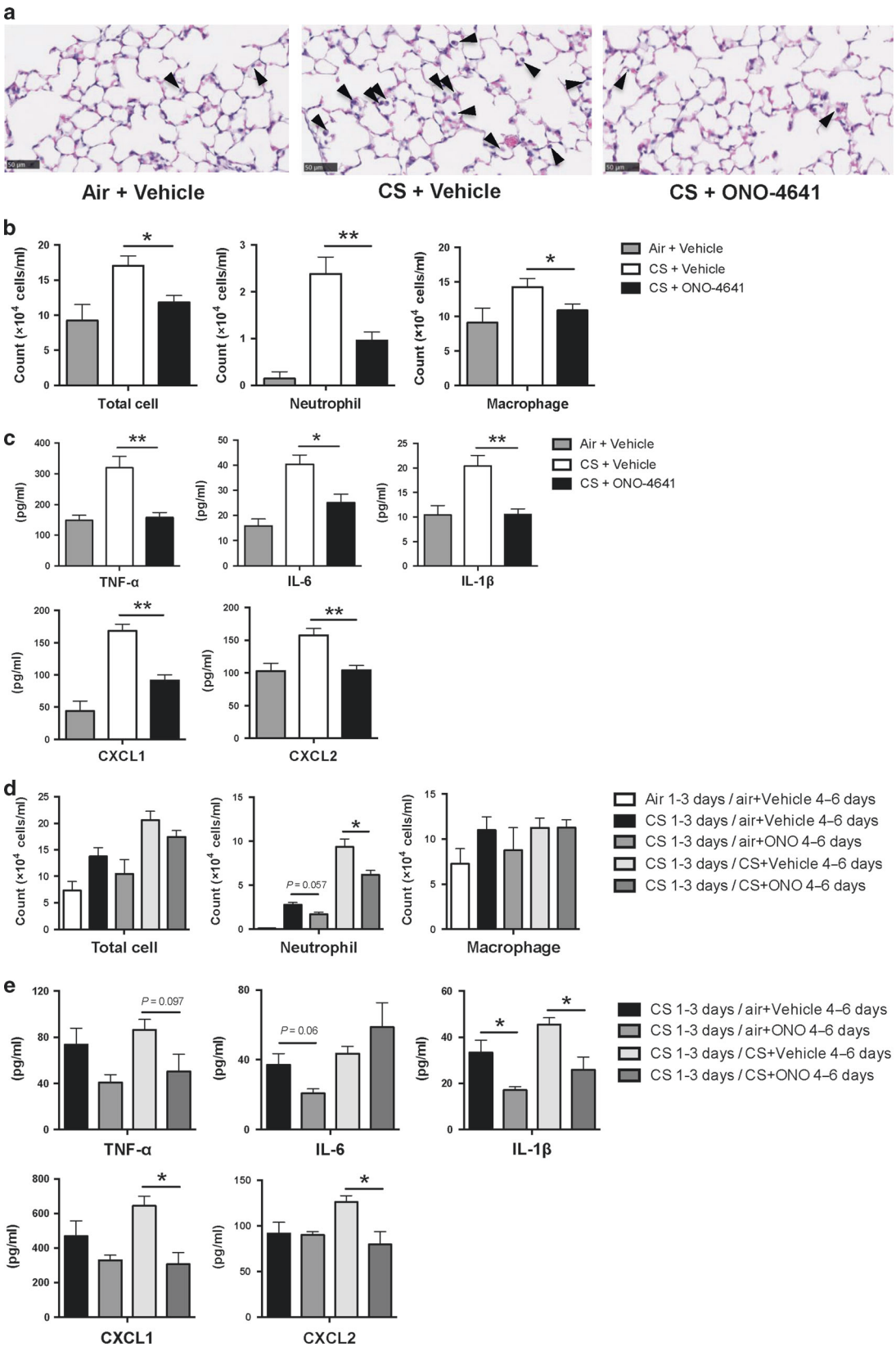

We observed that ONO-4641 treatment decreased the amount of peribronchovascular cell clusters in the CS-induced emphysema model and reduced the number lung lymphocytes expressing MMP-12 in the COPD exacerbation model. Previous studies have demonstrated that chronic inflammatory responses of T lymphocytes and B lymphocytes contribute to COPD pathogenesis.[5,44–46] In COPD patients, the total number of T lymphocytes and B lymphocytes in the lung parenchyma and peripheral and central airways is increased, particularly in those with severe disease.[5,44] Furthermore, $CD8^+$ T lymphocytes were reported to be

Fig. 3 Protective effects of ONO-4641 treatment in the mouse model of airway inflammation after short-term CS exposure. **a**–**c** Representative images of hematoxylin–eosin-stained lung sections 3 days after air or cigarette smoke (CS) exposure in vehicle- or ONO-4641-treated mice (**a**); numbers of total cells, neutrophils, and macrophages (**b**); and the levels of TNF-α IL-6, IL-1β, CXCL1, and CXCL2 (**c**) in BALF 3 days after CS exposure are shown ($n = 2$ in air exposure group, $n = 8$ in each CS exposure group). Data are presented as the mean ± SEM. Mice were exposed to CS for 60 min/day for the indicated periods. ONO-4641 or vehicle was intragastrically injected at 0.3 mg/kg once a day at 1 h before CS exposure for indicated days. Arrowheads denote infiltrated cells. Data are presented as the mean ± SEM. *$P < 0.05$. **$P < 0.01$. Scale bar, 50 μm. **d**, **e** Mice were exposed to room air or CS for 3 consecutive days with an additional 3 days of exposure to room air or CS. At days 4 to 6, vehicle or ONO-4641 was administered at 0.3 mg/kg once a day at 1 h before CS exposure for the indicated days in the Figure. The numbers of total cells, neutrophils, and macrophages (**d**) and the levels of TNF-α IL-6, IL-1β, CXCL1, and CXCL2 (**e**) in BALF at day 6 of the experiment are shown. ($n = 4–6$ in each group). Data are presented as the mean ± SEM. *$P < 0.05$

required for the development of CS-induced emphysema through the pathogenetic pathway in which IFN-gamma-inducible protein-10 (IP10/CXCL10) induces MMP-12 production.[45] B lymphocytes are also required for emphysema development in mice, as B lymphocyte-deficient mice were found to be protected from CS-induced emphysema.[46] Additionally, lymphocyte aggregates, also called lymphoid follicles, containing activated T lymphocytes and B lymphocytes were shown to be increased in human and mouse emphysema.[5,47] Indeed, we have confirmed the presence of aggregated lymphocytes in the lungs after CS-induced emphysema. We also found that their numbers were decreased by ONO-4641 treatment. Therefore, we speculate that ONO-4641-induced lymphocytopenia likely protects against emphysema progression.

Our studies indicated that ONO-4641-expanded $CD11b^+Gr\text{-}1^+$ cells seem, in some aspects, to have similar features of MDSCs, a heterogeneous population of myeloid progenitors and immature myeloid cells that suppress immune responses.[18] We confirmed that ONO-4641-expanded $CD11b^+Gr\text{-}1^+$ cell populations comprised two major classes of MDSCs: $CD11b^+Ly\text{-}6G^+Ly6C^{low}$ cells and $CD11b^+Ly\text{-}6G^-Ly\text{-}6C^+$ cells. We also showed that ONO-4641-expanded $CD11b^+Gr\text{-}1^+$ cells demonstrated specific immunoregulatory properties, including increased arginase activity and suppressive effects on T cell proliferation and IFN-γ and TNF-α production in macrophages. These immunoregulatory properties of ONO-4641-expanded $CD11b^+Gr\text{-}1^+$ cells may also contribute to decreased levels of inflammatory mediators in BALF from ONO-4641-treated mice. We also showed that ONO-4641-expanded $CD11b^+Gr\text{-}1^+$ cells exhibited higher expression of CD244, a marker reportedly expressed by granulocytic MDSCs at levels correlating with their immunosuppressive properties.[23] Indeed, by using this marker, we could distinguish ONO-4641-expanded $CD11b^+Gr\text{-}1^+$ cells from mature neutrophils.

For the ONO-4641-expanded $CD11b^+Ly\text{-}6G^-Ly\text{-}6C^+$ cells, it is necessary to distinguish monocytic MDSCs from M2 macrophages because several features including arginase expression, IL-10 production, reduced responsiveness to LPS stimulation, and reduced ability to activate T cell proliferation found in ONO-4641-expanded monocytic MDSCs are also typical of M2 macrophages.[48] However, ONO-4641-expanded $CD11b^+Gr\text{-}1^+$ cells also show induction of M1 marker genes (*Nos2*, *Tnfa*, *Il6*, and *Il1b*). In addition, ONO-4641-expanded $CD11b^+Gr1^+$ cells fulfill the definition of MDSCs;[49] ONO-4641-expanded cells show the typical phenotype of $CD11b^+Gr1^+$ cells and immunosuppressive activity of T cells, including not only inhibition of proliferation but also reduced IFN-γ production. These results indicate that ONO-4641-expanded $Ly\text{-}6G^-Ly\text{-}6C^+$ cells are not typical M2 macrophages but rather monocytic MDSCs.

In addition, we found that out of several tested S1PR1-selective agonists, ONO-4641 and CYM-5442, but not SEW2871, stimulated expansion of $CD11b^+Gr\text{-}1^+$ cells. CYM-5442 has been reported to be not only an S1PR1-selective agonist but also a functional S1PR1 antagonist, whereas SEW2871 has been reported to be an S1PR1 selective agonist.[22] Therefore, we speculate that the expansion of $CD11b^+Gr\text{-}1^+$ cells was induced through functional S1PR1 antagonism, which was associated with the exposure to CYM-5442 but not to SEW2871. We believe that functional S1PR suppression, rather than agonist effects, was crucial for the protective effects of long-term ONO-4641 treatment against emphysema progression.

We found that ONO-4641 treatment induced $CD11b^+Gr\text{-}1^+$ cell expansion in three different emphysema models: elastase-induced emphysema, CS-induced emphysema, and COPD exacerbation of elastase-induced emphysema. However, the roles of $CD11b^+Gr\text{-}1^+$ cell expansion in COPD are not entirely clear. A previous study demonstrated that current smoking activated circulating MDSCs in non-COPD smokers and COPD patients, as compared to MDSCs in individuals that never smoked. MDSC expansion was observed even after COPD patients quit smoking.[50] Another study showed that an increase in MDSCs correlated with elevated levels of T-regulatory cells or immunosuppressive cytokines in COPD patients.[51] In the present study, we observed expansion of $CD11b^+Gr\text{-}1^+$ cells after chronic CS exposure without ONO-4641 treatment ("CS + Vehicle" group in Fig. 6f, g), but not in elastase-induced emphysema (Fig. 4h). Based on these previous studies, although we did not evaluate the phenotype of $CD11b^+Gr1^+$ cells expanded after CS exposure (without ONO-4641 treatment), and these previous studies focused on MDSCs in peripheral blood but not in the lungs, we speculate that the CS-expanded $CD11b^+Gr1^+$ cell population also likely represented immunosuppressive and anti-inflammatory MDSC-like cells. We believe that CS-expanded MDSC-like cells failed to halt emphysema due to moderate (insufficient) levels of expansion, whereas more effective expansion of MDSC-like cells by ONO-4641 treatment could protect against emphysema progression in COPD.

Several limitations of the present study should be acknowledged. First, we did not confirm that the ONO-4641-expanded $CD11b^+Gr\text{-}1^+$ cells were genuine MDSCs, although we have demonstrated that ONO-4641-expanded $CD11b^+Gr\text{-}1^+$ cells show, in some aspects, an anti-inflammatory MDSC phenotype. Second, we did not evaluate the extent to which the effects of ONO-4641 on $CD11b^+Gr\text{-}1^+$ cell population expansion, lymphocytopenia, and ceramide levels contributed to the protective effects in our emphysema and COPD exacerbation models. As we confirmed the expansion of $CD11b^+Gr\text{-}1^+$ cell populations in these models and found that adoptive transfer of ONO-4641-expanded $CD11b^+Gr\text{-}1^+$ cells diminished progression of elastase-induced emphysema, we believe that expansion of the $CD11b^+Gr\text{-}1^+$ cell population likely plays a major role in ONO-4641 protective effects. Third, we did not determine whether the MDSC-like population could be also expanded by ONO-4641 treatment and whether ONO-4641 would also exhibit protective effects in patients with COPD in the clinical setting. As another S1PR modulator, fingolimod (FTY720), is already in clinical use for other diseases,[2] a clinical drug-repositioning study of ONO-4641 in COPD should resolve these issues in the near feature.

In conclusion, we have demonstrated that ONO-4641 attenuated murine pulmonary emphysema by expanding lung $CD11b^+Gr\text{-}1^+$ cell populations and inducing lymphocytopenia. The S1P receptor might therefore be a promising target for strategies aimed at ameliorating pulmonary emphysema progression. Further studies are required for a better understanding of the mechanisms underlying the beneficial effects of S1PR modulation in COPD.

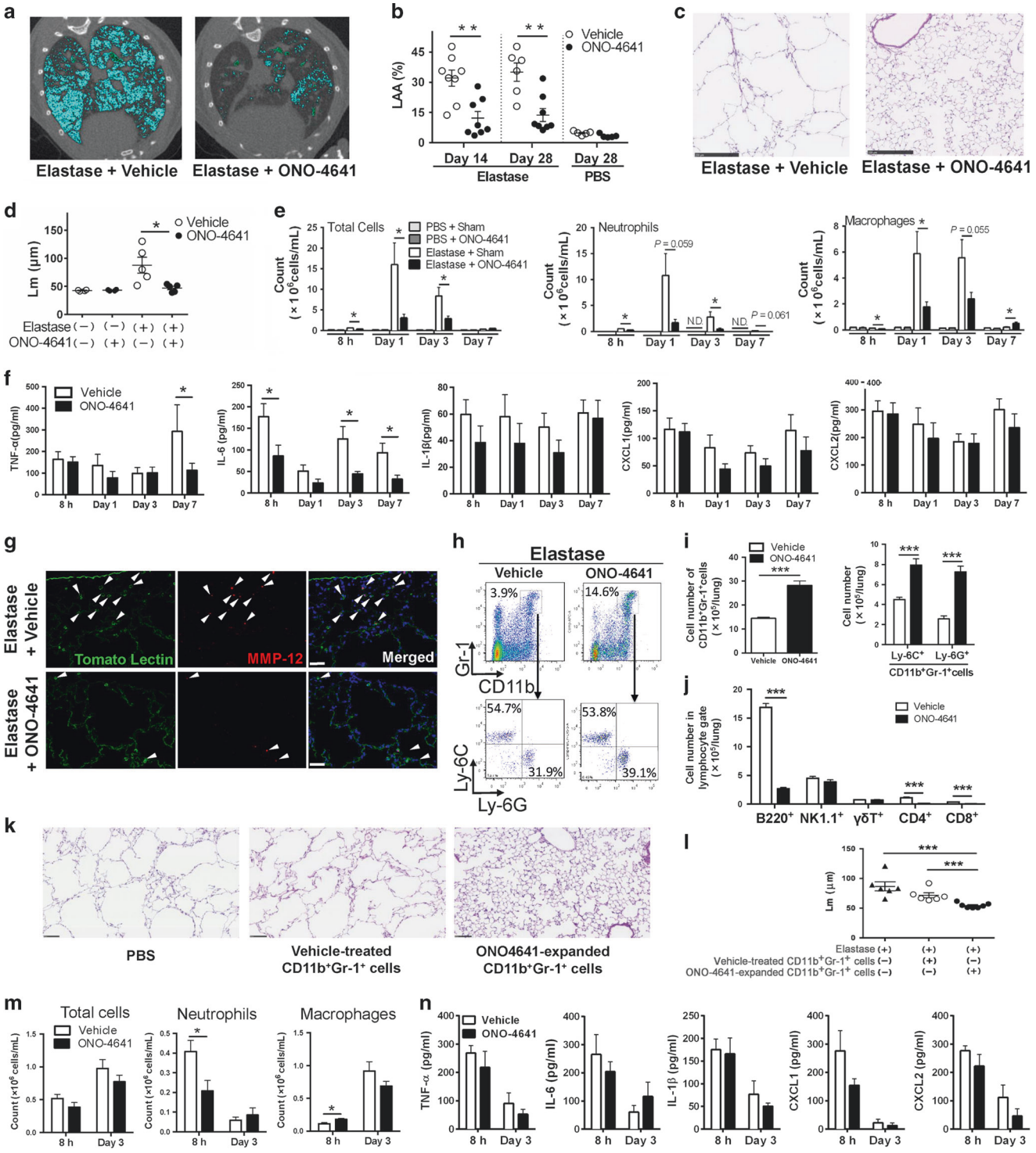

METHODS

Further information can be found in the Supplemental Methods.

Mice

Female WT C57BL/6 J mice (8−10 weeks old) were purchased from CLEA Japan (Tokyo, Japan). The Animal Use Committee at the Keio University School of Medicine approved all animal experiments (protocols No. 12109 and No. 2110).

Preparation and injection of ONO-4641 and other drugs

ONO-4641 was provided by Ono Pharmaceutical Co., Ltd (Osaka, Japan) and diluted with 0.5% methylcellulose. ONO-4641 or vehicle was intragastrically injected at 0.3 mg/kg once a day at 1 h before short-term or long-term CS exposure for the indicated periods.

In the elastase-induced emphysema model, ONO-4641 (0.3 mg/kg) or vehicle was intragastrically injected at 1 h before elastase injection, and then every 24 h for consecutive 14 days.

Fig. 4 Protective effects of ONO-4641 treatment against elastase-induced emphysema in mice. Mice were intratracheally injected with 5 U of porcine pancreatic elastase. ONO-4641 (0.3 mg/kg) or vehicle was intragastrically injected at 1 h before elastase injection, and then every 24 h for consecutive 14 days. **a** Representative micro-CT images of lung cross-sections in a mouse model of elastase-induced emphysema treated with vehicle or ONO-4641 (Day 28); the low-attenuation areas (LAAs, less than −700 Hounsfield units) are presented in blue. **b** LAA percentage in mice with elastase or PBS-treated emphysema that were administered vehicle or ONO-4641 at the indicated time points ($n = 6–8$ in the elastase-treated group, $n = 5$ in the PBS-treated group). Data are presented as the mean ± SEM. $^{**}P < 0.01$. **c** Histopathological examination of lung specimens from mice with elastase-treated emphysema that were administered vehicle or ONO-4641 (Day 28). Scale bar, 250 μm (**d**) Mean linear intercepts (Lm) were determined as the average of 10 randomly selected fields of each lung obtained from vehicle-treated or ONO-4641-treated mice 28 days after elastase or PBS injection ($n = 5$ in elastase-treated group, $n = 4$ in PBS-treated group). Data are presented as the mean ± SEM. $^{*}P < 0.05$. **e**, **f** Numbers of total cells, neutrophils, macrophages (**e**), and levels of TNF-α, IL-6, IL-1β, CXCL1, and CXCL2 (**f**) in BALF at the indicated time points after elastase injection ($n = 6–8$ in elastase-treated group, $n = 4–5$ in PBS-treated group). Data are presented as the mean ± SEM. $^{*}P < 0.05$. **g** Representative dual staining for tomato lectin and MMP-12 in the lungs of mice with elastase-treated emphysema that were administered vehicle or ONO-4641 (Day 7). Scale bar, 50 μm. **h**–**j** Representative two-parameter histograms (**h**), quantification of $CD11b^{+}Gr\text{-}1^{+}$ cells including $Ly\text{-}6C^{+}$ and $Ly\text{-}6G^{+}$ cells (**i**), and quantification of lymphocytes (**j**) in the lungs from mice intragastrically treated with vehicle or ONO-4641 (0.3 mg/kg) once a day for 7 days after elastase injection ($n = 5$ in each group). Data are presented as the mean ± SEM. $^{***}P < 0.001$. **k**, **l** Histopathological examination of lung specimens (**k**) and Lm (**l**) in elastase-treated mice 28 days after intravenous adoptive transfer of PBS, or vehicle-treated or ONO-4641-expanded $CD11b^{+}Gr\text{-}1^{+}$ cells ($n = 6$ or 7 in each group). **m**, **n** Numbers of total cells, neutrophils, and macrophages (**m**), and levels of TNF-α, IL-6, IL-1β, CXCL1, and CXCL2 (**n**) in BALF at the indicated time points after elastase injection with adaptive transfer of vehicle-treated or ONO-4641-expanded $CD11b^{+}Gr\text{-}1^{+}$ cells ($n = 3–5$). Data are presented as the mean ± SEM. $^{*}P < 0.05$. $^{***}P < 0.001$

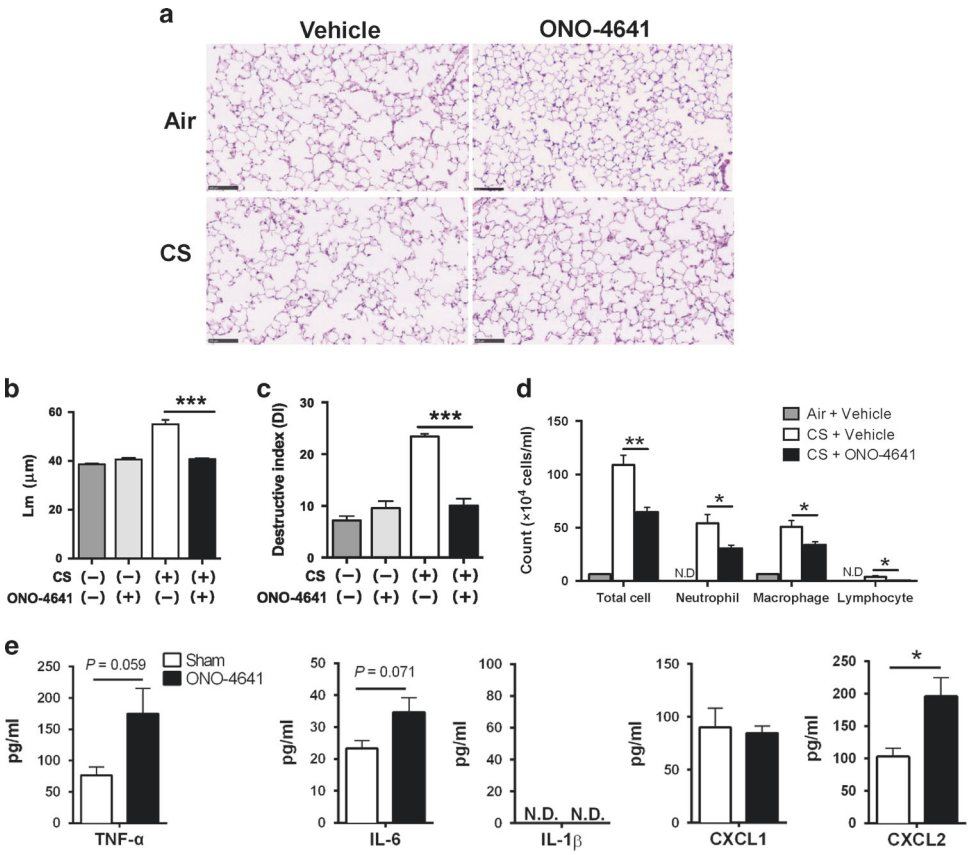

Fig. 5 Protective effects of ONO-4641 treatment against emphysema induced by long-term CS exposure in mice. **a**–**c** Representative images of hematoxylin/eosin-stained lung sections obtained 3 months after exposure to air or CS (60 min/day and 5 days/week over 3 months) in vehicle-treated and ONO-4641-treated (once a day at 1 h before CS exposure over 3 months) mice (**a**). Scale bar, 100 μm. Mean linear intercepts (Lm) were determined as averages of 10 randomly selected fields of each lung obtained from vehicle- or ONO-4641-treated mice euthanized 3 months after CS exposure (**b**) ($n = 2$ in air exposure group, $n = 5$ in each CS exposure group). Data are presented as the mean ± SEM. $^{***}P < 0.001$. Destructive index (DI) values representing alveolar destruction are shown (**c**). **d** Numbers of total cells, neutrophils, macrophages, and lymphocytes in BALF at 3 months after exposure to air or CS of vehicle-treated or ONO-4641-treated mice ($n = 3$ in air-exposed group, $n = 4$ in each CS-exposed group). Data are presented as the mean ± SEM. $^{*}P < 0.05$. $^{**}P < 0.01$. **e** Levels of TNF-α, IL-6, IL-1β, CXCL1, and CXCL2 in BALF 3 months after exposure to CS (60 min/day and 5 days/week over 3 months) in vehicle-treated and ONO-4641-treated (once a day at 1 h before CS exposure over 3 months) mice ($n = 4$ in each group). Data are presented as the mean ± SEM

In elastase-treated mice after pneumococcal infection, ONO-4641 (0.3 mg/kg) or vehicle was intragastrically injected at 1 h before pneumococcal infection, and then every 24 h for consecutive 14 days. The dose of ONO-4641 was determined on the basis of previous reports.[17] C-8 ceramide-1-phosphate and C-16 ceramide-1-phosphate (Cayman Chemical) were intragastrically injected at 40 and 50 μg/kg, respectively, as previously described.[21] SEW2871 (Cayman Chemical) and CYM-5442 (R&D

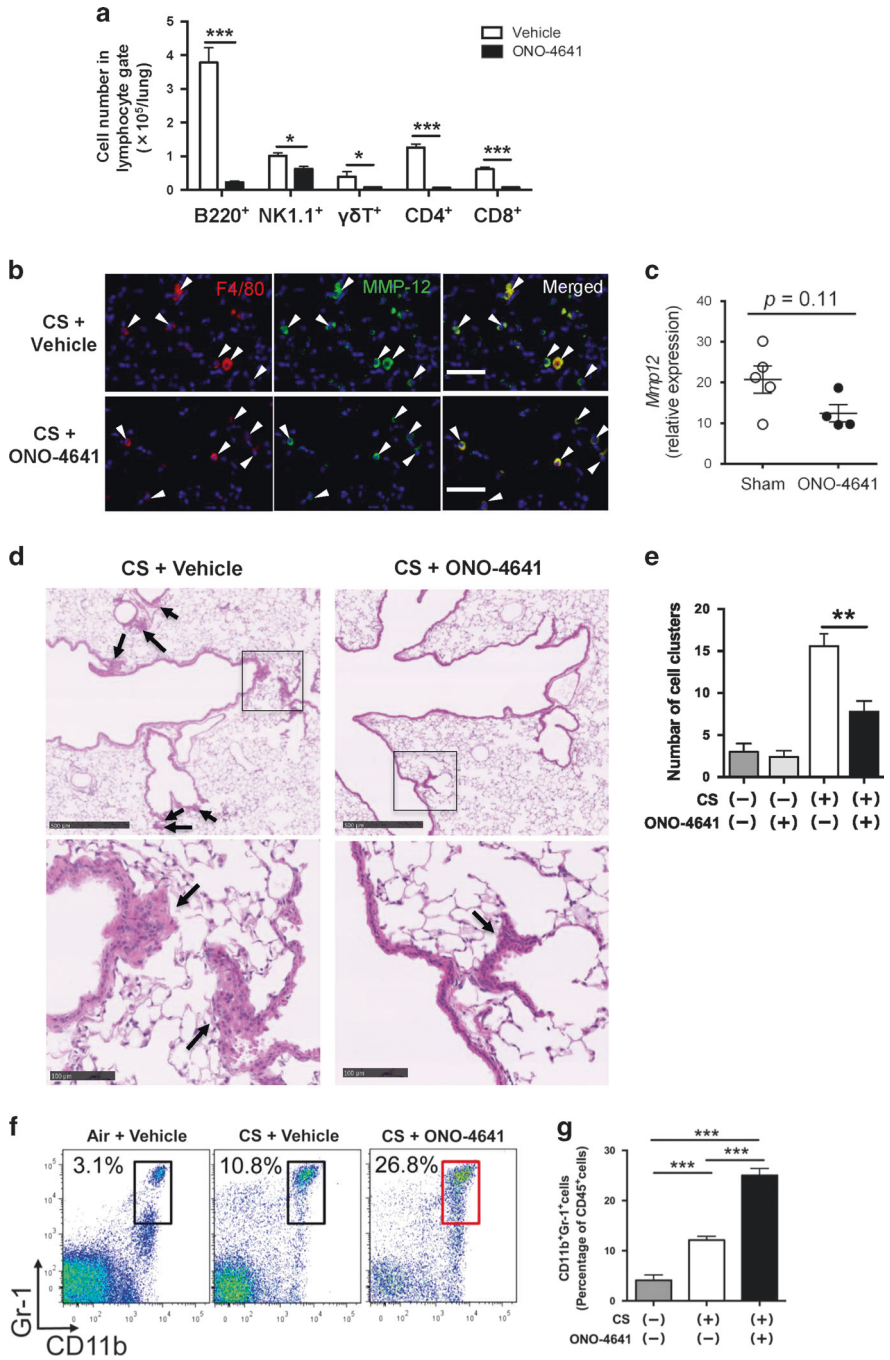

Fig. 6 Lymphocytopenia and expansion of lung CD11b$^+$Gr-1$^+$ cells by ONO-4641 in emphysema induced by long-term CS exposure. **a** CS exposure was performed for 60 min/day and 5 days/week over 3 months. Quantification of indicated major lymphocyte populations in the lungs from mice treated intragastrically with vehicle or ONO-4641 (0.3 mg/kg) once a day at 1 h before CS exposure for 3 months ($n = 4–5$ in each group). Data are presented as the mean ± SEM. *$P < 0.05$. ***$P < 0.001$. **b**, **c** Representative dual staining for F4/80 and MMP-12 (**b**) in the lungs of mice at 3 months after CS exposure. Scale bar, 50 μm. *Mmp12* mRNA expression (**c**) in the lungs of vehicle or ONO-4641-treated mice was measured by quantitative real-time PCR ($n = 4–5$ in each group). Data are presented as the mean ± SEM. **d** Enhancement of peribronchovascular cell cluster formation in CS-exposed lungs. Representative hematoxylin–eosin staining of lung sections 3 months after exposure of the lungs to CS with vehicle or ONO-4641 treatment (0.3 mg/kg) once a day at 1 h before CS exposure for 3 months ($n = 4$ in each group). Arrows indicate sites of peribronchovascular cell cluster formation. Scale bar, 500 μm (upper panel, lower magnification) and 100 μm (lower panel, higher magnification). **e** Number of peribronchovascular cell clusters in lung tissue at 3 months after air or CS exposure in mice treated with vehicle or ONO-4641 ($n = 2$ in each air-exposed group, $n = 5$ in each CS-exposed group). Peribronchovascular cell clusters were counted in all fields of H&E stained lung coronal sections with the largest surface in each mouse. Data are presented as the mean ± SEM. **$P < 0.01$. **f**, **g** Representative two-parameter histograms (**f**), and quantification of CD11b$^+$Gr-1$^+$ cells (**g**) in the lungs from mice treated intragastrically with vehicle or ONO-4641 at 3 months after CS exposure ($n = 4–5$ in each group). Data are presented as the mean ± SEM. ***$P < 0.001$

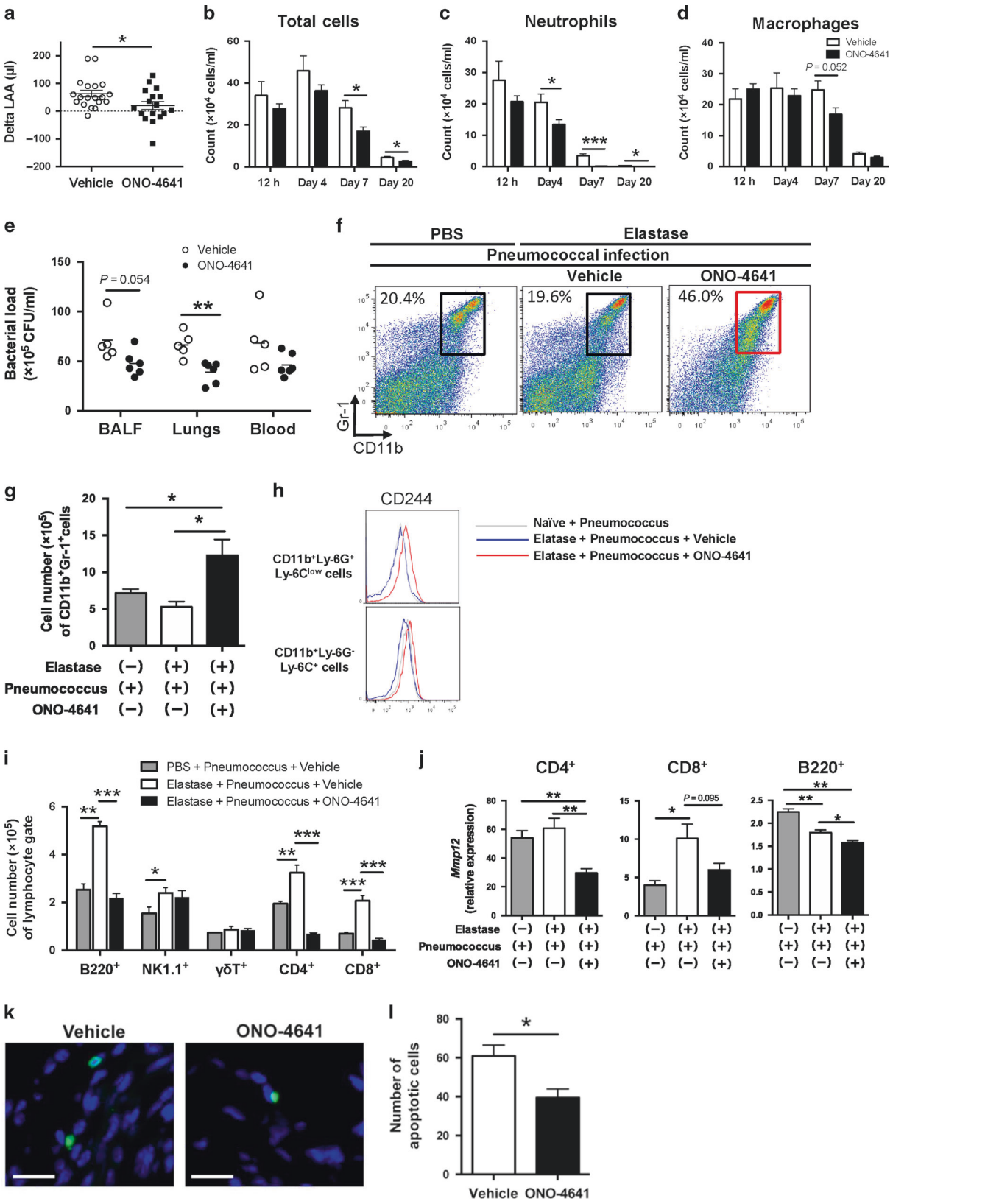

Systems, Minneapolis, MN) were intraperitoneally injected once a day for the indicated periods at 1 mg/kg and 3 mg/kg, respectively, according to previous reports.[38,52,53]

For inhibition of the ERK pathway, the MEK/ERK inhibitor U0126 (Promega, Madison, WI; 5 mg/kg) or vehicle was intraperitoneally injected 30 min before ONO-4641 treatment once a day for seven consecutive days based on a previous report.[54]

Fig. 7 Protective effects of ONO-4641 treatment against emphysema progression in elastase-treated mice after pneumococcal infection. **a** Change in low-attenuation area (delta LAA) volumes in the lungs of pneumococcus-infected mice with elastase-induced emphysema that were treated with vehicle or ONO-4641 (0.3 mg/kg) once a day at 1 h before pneumococcal infection, and then every 24 h for consecutive 14 days. Delta LAA volume was calculated by subtracting LAA volume before infection from the volume at 14 days after infection. ($n = 17–19$ in each group). Data are presented as the mean ± SEM. $^*P < 0.05$. **b**–**d** Numbers of total cells (**b**), neutrophils (**c**), and macrophages (**d**) in BALF at indicated time points after pneumococcal infection in mice with elastase-induced emphysema that were treated with vehicle or ONO-4641 (0.3 mg/kg) once a day at 1 h before pneumococcal infection, and then every 24 h for the indicated periods. ($n = 5–6$ in each group). Data are presented as the mean ± SEM. $^*P < 0.05$; $^{***}P < 0.001$. **e** BALF, lysate of the whole right lower lung, and blood obtained at day 4 after pneumococcal infection were serially diluted and plated on trypticase soy agar plates. Bacterial loads are expressed as colony-forming units (CFUs) per milliliter. ($n = 5–6$ in each group). Data are presented as the mean ± SEM. $^{**}P < 0.01$. **f**–**h** Representative two-parameter histograms (**f**) and quantification of $CD11b^+Gr\text{-}1^+$ cells (**g**), and representative histogram of CD244 expression by vehicle-expanded and ONO-4641-expanded $CD11b^+Gr\text{-}1^+$ cells (**h**) in elastase-treated mice at day 4 after pneumococcal infection ($n = 4$ in each group). **i**, **j** Lymphocyte subsets (**i**) and *Mmp12* expression in $CD4^+$ and $CD8^+$ T lymphocytes and $B220^+$ B lymphocytes (**j**) in lungs from pneumococcus-infected mice with elastase-induced emphysema that were treated with vehicle or ONO-4641 (Day 4; $n = 4–6$ in each group). Data are presented relative to expression levels in $CD4^+$ cells, $CD8^+$ cells, and $B220^+$ cells in lungs of naive mice as the mean ± SEM. $^*P < 0.05$; $^{**}P < 0.01$; $^{***}P < 0.001$. **k**, **l** Representative TUNEL staining of the lungs (**h**) and the number of apoptotic cells (**i**) from pneumococcus-infected mice with elastase-induced emphysema that were treated with vehicle or ONO-4641 (0.3 mg/kg) once a day at 1 h before pneumococcal infection, and then every 24 h for 14 days. (Day 14; scale bar, 20 μm; $n = 7–9$ in each group). Data are presented as the mean ± SEM. $^*P < 0.05$

Flow cytometry and sorting

Single-cell suspensions of spleens and lungs were blocked with an antibody against CD16/CD32 (Thermo Fisher Scientific, Waltham, MA) for 10 min and incubated with the primary antibody for 15 min. The stained cells were processed by flow cytometry on a BD FACS Aria II system (BD Biosciences, San Jose, CA) or MoFlo XDP (Beckman Coulter, Brea, CA) as previously described.[55]

Elastase-induced emphysema and pneumococcal infection mouse model

In the elastase-induced emphysema model, mice were intratracheally injected with 5 U of porcine pancreatic elastase (Elastin Products, Owensville, MO).[39] For adoptive transfer experiments, lung $CD11b^+Gr\text{-}1^+$ cells (1×10^6/mouse) in 0.1 mL of PBS sorted from ONO-treated or vehicle-treated mice were intravenously transferred into mice via tail vein injection 1 h before elastase injection.

In the COPD exacerbation model, the mice were intranasally inoculated with 1×10^7 colony-forming units (CFUs) of *Streptococcus pneumoniae* serotype 6 C at 4 weeks after elastase injection. Clinical specimens were isolated and suspended in 50 μL of sterile PBS as previously described.[39]

Mouse models of lung inflammation due to acute and chronic CS exposure

Lung inflammation was induced by CS exposure as previously described.[40] In brief, mice were exposed to mainstream CS generated from commercially available filtered cigarettes (Marlboro; Philip Morris, New York, NY) (12 mg tar/1.0 mg nicotine). CS inhalation was achieved by using a SIS-CS system (Shibata Scientific Technology, Tokyo, Japan).

For the acute CS exposure model, mice were exposed to CS for 60 min/day for the indicated periods. For the chronic CS exposure model, mice were exposed to CS for 60 min/day and 5 days/week over 3 months. Mice were killed 3 months after CS exposure.

Micro-computed tomography

A micro-computed tomography (CT) system R_mCT2 (Rigaku, Tokyo, Japan) and a Lexus 64 workstation (AZE Ltd., Tokyo, Japan) were used for imaging 14 and 28 days after elastase treatment. We arbitrarily established the threshold for LAA as less than −700 HU in the elastase-induced emphysema model.[56]

Bronchoalveolar lavage

We performed BALF collection and determined total and differential cell counts as previously described.[57]

Enzyme-linked immunosorbent assay

TNF-α, IL-6, IL-1β, CXCL1, CXCL2, and CCL2 levels in BALF were measured using enzyme-linked immunosorbent assay kits (R&D Systems) as previously described.[58]

Quantitative real-time PCR

Total RNA from lung tissue or sorted cells was extracted, reverse transcribed, and subjected to quantitative real-time PCR.[39] The primer sequences for each target gene are provided in Supplementary Table 1.

Histopathological examination and immunofluorescence

Lungs were fixed by intratracheal instillation of 4% paraformaldehyde at a constant pressure of 20 cm H_2O. Paraffin-embedded 3-μm sections of the lung were stained with hematoxylin–eosin. The detailed protocol for the immunofluorescence studies is provided in the Supplemental Methods.

Lung morphometric analysis

To measure airspace size and alveolar destruction, the mean linear intercept (Lm) and destructive index (DI) were determined in 10 randomly selected fields per lung specimen for each mouse as previously described.[40,59]

Bacterial load

The right lower lung lobes were harvested and homogenized with 1 mL of PBS. The lung homogenate, blood, and BALF were serially diluted with sterile PBS. Equal volumes of each dilution were applied to trypticase soy agar plates containing 5% sheep blood (BD Trypticase Soy Agar II with 5% Sheep Blood; BD Diagnostics, San Jose, CA) and incubated overnight at 37 °C. On the next day, bacterial colonies were counted and expressed as CFUs per mL of solution as previously described.[60]

Statistics

Data are expressed as the mean ± SEM. Statistical significance of differences between groups was assessed using unpaired Student's *t*-test or analysis of variance followed by the post hoc Tukey test for multiple comparisons, or log-rank test for survival using Prism 6 software (GraphPad Software; San Diego, CA). All statistical analyses were conducted with a significance level of $\alpha = 0.05$ ($P < 0.05$).

ACKNOWLEDGEMENTS

We thank Professor Mitsuru Murata, Mr. Yasuhiro Katono, Ms. Miyuki Yamamoto, Ms. Mikiko Shibuya, and Dr. Junko Hamamoto for their research assistance, and Mr. Akira

Sonoda (Keio-Med Open Access Facility, Keio University School of Medicine) for his skilled technical assistance.

AUTHOR CONTRIBUTIONS

T.A., M.I., and T.B. designed the experiments. T.A., H.N., A.E.H., and S.K. conducted the experiments. S.S., K.Y., T.K., S.O., H.K., S.T., A.E.H., N.H. assisted in designing the experiments and critically reviewed the manuscript. T.A. and M.I. wrote the manuscript. A.K. and T.B. supervised the project and critically reviewed the manuscript.

ADDITIONAL INFORMATION

The online version of this article (https://doi.org/10.1038/s41385-018-0077-5) contains supplementary material, which is available to authorized users.

Competing interests: T.A., M.I., and T.B. received research grants from Ono Pharmaceutical Co., Ltd. T.K. and T.H. are employees of Ono Pharmaceutical Co., Ltd. The remaining authors declare no competing interests.

REFERENCES

1. Vestbo, J. et al. Global strategy for the diagnosis, management, and prevention of chronic obstructive pulmonary disease: GOLD executive summary. *Am. J. Respir. Crit. Care Med.* **187**, 347–365 (2013).
2. Guarnera, C., Bramanti, P. & Mazzon, E. Comparison of efficacy and safety of oral agents for the treatment of relapsing-remitting multiple sclerosis. *Drug Des. Devel Ther.* **11**, 2193–2207 (2017).
3. Pauwels, R. A. & Rabe, K. F. Burden and clinical features of chronic obstructive pulmonary disease (COPD). *Lancet* **364**, 613–620 (2004).
4. Wedzicha, J. A. & Seemungal, T. A. COPD exacerbations: defining their cause and prevention. *Lancet* **370**, 786–796 (2007).
5. Hogg, J. C. et al. The nature of small-airway obstruction in chronic obstructive pulmonary disease. *N. Engl. J. Med.* **350**, 2645–2653 (2004).
6. Taraseviciene-Stewart, L. & Voelkel, N. F. Molecular pathogenesis of emphysema. *J. Clin. Invest.* **118**, 394–402 (2008).
7. Petrache, I. & Berdyshev, E. V. Ceramide signaling and metabolism in pathophysiological states of the lung. *Annu. Rev. Physiol.* **78**, 463–480 (2016).
8. Hannun, Y. A. Functions of ceramide in coordinating cellular responses to stress. *Science* **274**, 1855–1859 (1996).
9. Scarpa, M. C. et al. Ceramide expression and cell homeostasis in chronic obstructive pulmonary disease. *Respiration* **85**, 342–349 (2013).
10. Petrache, I. et al. Ceramide upregulation causes pulmonary cell apoptosis and emphysema-like disease in mice. *Nat. Med.* **11**, 491–498 (2005).
11. Diab, K. J. et al. Stimulation of sphingosine 1-phosphate signaling as an alveolar cell survival strategy in emphysema. *Am. J. Respir. Crit. Care. Med.* **181**, 344–352 (2010).
12. Bowler, R. P. et al. Plasma sphingolipids associated with chronic obstructive pulmonary disease phenotypes. *Am. J. Respir. Crit. Care. Med.* **191**, 275–284 (2015).
13. Kunkel, G. T., Maceyka, M., Milstien, S. & Spiegel, S. Targeting the sphingosine-1-phosphate axis in cancer, inflammation and beyond. *Nat. Rev. Drug Discov.* **12**, 688–702 (2013).
14. Peng, X. et al. Protective effects of sphingosine 1-phosphate in murine endotoxin-induced inflammatory lung injury. *Am. J. Respir. Crit. Care. Med.* **169**, 1245–1251 (2004).
15. Walsh, K. B. et al. Suppression of cytokine storm with a sphingosine analog provides protection against pathogenic influenza virus. *Proc. Natl Acad. Sci. USA* **108**, 12018–12023 (2011).
16. Mandala, S. et al. Alteration of lymphocyte trafficking by sphingosine-1-phosphate receptor agonists. *Science* **296**, 346–349 (2002).
17. Komiya, T. et al. Efficacy and immunomodulatory actions of ONO-4641, a novel selective agonist for sphingosine 1-phosphate receptors 1 and 5, in preclinical models of multiple sclerosis. *Clin. Exp. Immunol.* **171**, 54–62 (2013).
18. Gabrilovich, D. I. & Nagaraj, S. Myeloid-derived suppressor cells as regulators of the immune system. *Nat. Rev. Immunol.* **9**, 162–174 (2009).
19. Huu, D. L. et al. FTY720 ameliorates murine sclerodermatous chronic graft-versus-host disease by promoting expansion of splenic regulatory cells and inhibiting immune cell infiltration into skin. *Arthritis Rheum.* **65**, 1624–1635 (2013).
20. Liu, G. et al. Targeting S1P1 receptor protects against murine immunological hepatic injury through myeloid-derived suppressor cells. *J. Immunol.* **192**, 3068–3079 (2014).
21. Baudiss, K. et al. Ceramide-1-phosphate inhibits cigarette smoke-induced airway inflammation. *Eur. Respir. J.* **45**, 1669–1680 (2015).
22. Li, C., Li, J. N., Kays, J., Guerrero, M. & Nicol, G. D. Sphingosine 1-phosphate enhances the excitability of rat sensory neurons through activation of sphingosine 1-phosphate receptors 1 and/or 3. *J. Neuroinflamm.* **12**, 70 (2015).
23. Youn, J. I., Collazo, M., Shalova, I. N., Biswas, S. K. & Gabrilovich, D. I. Characterization of the nature of granulocytic myeloid-derived suppressor cells in tumor-bearing mice. *J. Leukoc. Biol.* **91**, 167–181 (2012).
24. Haile, L. A., Gamrekelashvili, J., Manns, M. P., Korangy, F. & Greten, T. F. CD49d is a new marker for distinct myeloid-derived suppressor cell subpopulations in mice. *J. Immunol.* **185**, 203–210 (2010).
25. Talmadge, J. E. & Gabrilovich, D. I. History of myeloid-derived suppressor cells. *Nat. Rev. Cancer* **13**, 739–752 (2013).
26. Gutknecht, M. F. & Bouton, A. H. Functional significance of mononuclear phagocyte populations generated through adult hematopoiesis. *J. Leukoc. Biol.* **96**, 969–980 (2014).
27. Ding, Y. et al. CD40 controls CXCR5-induced recruitment of myeloid-derived suppressor cells to gastric cancer. *Oncotarget* **6**, 38901–38911 (2015).
28. Bronte, V. et al. Identification of a CD11b(+)/Gr-1(+)/CD31(+) myeloid progenitor capable of activating or suppressing CD8(+) T cells. *Blood* **96**, 3838–3846 (2000).
29. Movahedi, K. et al. Identification of discrete tumor-induced myeloid-derived suppressor cell subpopulations with distinct T cell-suppressive activity. *Blood* **111**, 4233–4244 (2008).
30. Goedegebuure, P. et al. Myeloid-derived suppressor cells: general characteristics and relevance to clinical management of pancreatic cancer. *Curr. Cancer Drug Targets* **11**, 734–751 (2011).
31. Noman, M. Z. et al. PD-L1 is a novel direct target of HIF-1alpha, and its blockade under hypoxia enhanced MDSC-mediated T cell activation. *J. Exp. Med.* **211**, 781–790 (2014).
32. Jablonski, K. A. et al. Novel markers to delineate murine M1 and M2 macrophages. *PLoS ONE* **10**, e0145342 (2015).
33. Odegaard, J. I. et al. Alternative M2 activation of Kupffer cells by PPARdelta ameliorates obesity-induced insulin resistance. *Cell Metab.* **7**, 496–507 (2008).
34. Gordon, S. & Martinez, F. O. Alternative activation of macrophages: mechanism and functions. *Immunity* **32**, 593–604 (2010).
35. Ishii, M. et al. Epigenetic regulation of the alternatively activated macrophage phenotype. *Blood* **114**, 3244–3254 (2009).
36. Liao, X. et al. Kruppel-like factor 4 regulates macrophage polarization. *J. Clin. Invest.* **121**, 2736–2749 (2011).
37. Brunkhorst, R., Vutukuri, R. & Pfeilschifter, W. Fingolimod for the treatment of neurological diseases-state of play and future perspectives. *Front. Cell. Neurosci.* **8**, 283 (2014).
38. Cheng, Q. et al. The S1P1 receptor-selective agonist CYM-5442 reduces the severity of acute GVHD by inhibiting macrophage recruitment. *Cell. Mol. Immunol.* **12**, 681–691 (2015).
39. Takahashi, S. et al. Pneumococcal infection aggravates elastase-induced emphysema via matrix metalloproteinase 12 overexpression. *J. Infect. Dis.* **213**, 1018–1030 (2016).
40. Sasaki, M. et al. Evaluation of cigarette smoke-induced emphysema in mice using quantitative micro-computed tomography. *Am. J. Physiol. Lung Cell. Mol. Physiol.* **308**, L1039–L1045 (2015).
41. Tanabe, N. et al. Impact of exacerbations on emphysema progression in chronic obstructive pulmonary disease. *Am. J. Respir. Crit. Care Med.* **183**, 1653–1659 (2011).
42. Proia, R. L. & Hla, T. Emerging biology of sphingosine-1-phosphate: its role in pathogenesis and therapy. *J. Clin. Invest.* **125**, 1379–1387 (2015).
43. Natarajan, V. et al. Sphingosine-1-phosphate, FTY720, and sphingosine-1-phosphate receptors in the pathobiology of acute lung injury. *Am. J. Respir. Cell. Mol. Biol.* **49**, 6–17 (2013).
44. Grumelli, S. et al. An immune basis for lung parenchymal destruction in chronic obstructive pulmonary disease and emphysema. *PLoS Med.* **1**, e8 (2004).
45. Maeno, T. et al. CD8+T Cells are required for inflammation and destruction in cigarette smoke-induced emphysema in mice. *J. Immunol.* **178**, 8090–8096 (2007).
46. John-Schuster, G. et al. Cigarette smoke-induced iBALT mediates macrophage activation in a B cell-dependent manner in COPD. *Am. J. Physiol. Lung Cell. Mol. Physiol.* **307**, L692–L706 (2014).
47. Polverino, F., Seys, L. J., Bracke, K. R. & Owen, C. A. B cells in chronic obstructive pulmonary disease: moving to center stage. *Am. J. Physiol. Lung Cell. Mol. Physiol.* **311**, L687–L695 (2016).
48. Sica, A. & Mantovani, A. Macrophage plasticity and polarization: in vivo veritas. *J. Clin. Invest.* **122**, 787–795 (2012).
49. Bronte, V. et al. Recommendations for myeloid-derived suppressor cell nomenclature and characterization standards. *Nat. Commun.* **7**, 12150 (2016).
50. Scrimini, S. et al. Differential effects of smoking and COPD upon circulating myeloid derived suppressor cells. *Respir. Med.* **107**, 1895–1903 (2013).

51. Kalathil, S. G. et al. T-regulatory cells and programmed death 1+T cells contribute to effector T-cell dysfunction in patients with chronic obstructive pulmonary disease. *Am. J. Respir. Crit. Care Med.* **190**, 40–50 (2014).
52. Awad, A. S. et al. Chronic sphingosine 1-phosphate 1 receptor activation attenuates early-stage diabetic nephropathy independent of lymphocytes. *Kidney Int.* **79**, 1090–1098 (2011).
53. Mathew, B. et al. Role of sphingolipids in murine radiation-induced lung injury: protection by sphingosine 1-phosphate analogs. *FASEB J.* **25**, 3388–3400 (2011).
54. Chialda, L., Zhang, M., Brune, K. & Pahl, A. Inhibitors of mitogen-activated protein kinases differentially regulate costimulated T cell cytokine production and mouse airway eosinophilia. *Respir. Res.* **6**, 36 (2005).
55. Namkoong, H. et al. Clarithromycin expands CD11b+Gr-1+cells via the STAT3/Bv8 axis to ameliorate lethal endotoxic shock and post-influenza bacterial pneumonia. *PLoS Pathog.* **14**, e1006955 (2018).
56. Artaechevarria, X. et al. Evaluation of micro-CT for emphysema assessment in mice: comparison with non-radiological techniques. *Eur. Radiol.* **21**, 954–962 (2011).
57. Yagi, K. et al. Histone deacetylase inhibition protects mice against lethal postinfluenza pneumococcal infection. *Crit. Care Med.* **44**, e980–e987 (2016).
58. Asami, T. et al. Anti-inflammatory roles of mesenchymal stromal cells during acute Streptococcus pneumoniae pulmonary infection in mice. *Cytotherapy* **20**, 302–313 (2018).
59. Saetta, M. et al. Destructive index: a measurement of lung parenchymal destruction in smokers. *Am. Rev. Respir. Dis.* **131**, 764–769 (1985).
60. Ishii, M. et al. CRTH2 is a critical regulator of neutrophil migration and resistance to polymicrobial sepsis. *J. Immunol.* **188**, 5655–5664 (2012).